Blockade of Interaction of α9 Integrin with its Ligands Hinders the Formation of Granulation in Cutaneous Wound Healing

Yosuke Nakayama[1], Shigeyuki Kon[1], Daisuke Kurotaki[1], Junko Morimoto[1], Yutaka Matsui[2], and Toshimitsu Uede[1]*.

Running title: Role of α9 integrin in cutaneous wound healing

[1]Devision of Molecular Immunology, [2]Department of Matrix Medicine, Institute for Genetic Medicine, Hokkaido University. Kita-15, Nishi-7, Kita-ku, Sapporo, 060-0815, Japan

*All correspondence should be addressed to Dr. Toshimitsu Uede, Division of Molecular Immunology, Institute for Genetic Medicine, Hokkaido University. Kita-15, Nishi-7, Kita-ku, Sapporo, 060-0815, Japan. E-mail:toshi@igm.hokudai.ac.jp

Abstract

The wound healing is a complex process consisting of inflammatory reaction, proliferation of mesenchymal cells, and formation and contraction of granulation tissue. The integrin receptors play crucial roles in this process. Recently, α9 integrin has also been detected on keratinocytes within wound sites. However, its functional significance at various wound healing processes was not fully elucidated. To address the role of α9 integrin in wound healing process, we made a full-thickness skin excisional wound and treated mice with anti-α9 integrin antibody. It has been shown that wound healing process was divided into three distinct phases; first re-epithelialization phase, second phase of granulation tissue formation, and followed by final phase of contraction of granulation tissue. We found that contraction of granulation tissue was not impaired by blocking the interaction of α9 integrin with its ligands, indicating that α9 integrin is not involved in myofibroblast differentiation. Of note, formation of granulation tissue as characterized by dense vimentin and CD31 positive area was impaired. The hindrance of granulation tissue formation is due to the inhibition of adhesion and migration of α9 integrin positive dermal fibroblasts. In conclusion, α9 integrin is involved in the formation of granulation tissue via regulating migration and adhesion of dermal fibroblasts in the full-thickness skin excisional wound model.

KEYWORDS: integrin; fibroblast; wound healing; osteopontin; tenascin-C

After skin injury, a dynamic wound healing process takes place. Wound healing process consists of an initial inflammatory response followed by re-epithelialization of wound area, formation of granulation tissue, accompanying neovascularization and wound contraction.[1, 2] This wound healing process is tightly coordinated by the interaction of cells with their surrounding extracellular matrix (ECM) proteins and growth factors.[3-5] The ECM, initially thought to act simply as a scaffold for cell adhesion, however, is now proved to be a dynamic structure, continually remodeling in response to various stimuli. The alterations in the composition of ECM, then provides signals into adjacent cells via cell surface receptors. Thus, interaction of ECM with cells via cell surface receptors such as integrins regulates cell shape, proliferation, intracellular signaling and differentiation, that are critical for maintaining normal tissue function and wound healing process.[3]

Indeed, it has been reported that various integrins play a critical role during the process of wound healing. For example, αvβ3 integrin is important for angiogenesis,[6, 7] and many of integrins, such as α3β1, α5β1 and α6β4 are shown to be involved in migration of keratinocytes into wound site.[8, 9] In addition, it became clear that among numerous ECM proteins, there is a group of secreted ECM proteins, that are important during development, but expression of those ECM in the adult is typically restricted to would repair and remodeling tissue. These proteins are designated as `matricellular proteins` including thrombospondins, connective tissue growth factors, osteopontin (OPN), and tenascin-C (TN-C). Matricellular proteins interact with integrin or modulate the activity of growth factors, and the structural components of classical ECM such as collagen.[10] Many studies

have focused on the role of matricellular proteins during wound healing and these studies have been done using matricellular protein gene-null mice.[11] In thrombospondin-2-null mice, full-thickness excisional wounds healed at an accelerated rate and resolved with minimal scarring as compared with those in wild-type mice.[12] On the other hand, absence of a single gene such as OPN or TN-C did not display any alteration in the rate of healing except minor histological abnormalities, suggesting that these genes have redundancies.[13, 14] Indeed, absence of two genes of matricellular proteins resulted in significant phenotypic alterations in would healing.[15, 16] In this regard, it should be noted that OPN and TN-C share α9β1 integrin as a common receptor.[17, 18] It has been also reported that EDA/EIIIA segment of fibronectin is expressed during the granulation tissue phase of wound healing and that it, too, is a ligand for α9β1 integrin.[19-22] Thus, it is interesting to examine whether α9β1 integrin plays a pivotal role during the wound healing process. However, because of the early postnatal mortality of α9-deficient mice,[23] a role of α9 integrin during the healing process of full-thickness skin wounds in mice still remains unclear. To address whether and how α9β1 integrin is involved in the wound healing process, we took advantage of using inhibitory anti-α9β1 integrin antibody (clone: 55A2C) in full-thickness skin excisional wound model.

Materials and methods

Animals

C57BL/6 mice were purchased from Japan SLC (Hamamatsu, Japan). All mice were housed in a specific pathogen-free barrier facility and screened regularly for pathogens. All studies and procedures were approved by the Committee on Animal Experimentation of Institute for Genetic Medicine, Hokkaido University.

Anti murine α9 integrin antibody

Hamster monoclonal antibodies against murine α9 integrin were developed. To block the function of α9 integrin, we used anti-α9 integrin antibody (clone: 55A2C) which has an inhibitory effect on the interaction between α9 integrin and its ligands including OPN and TN-C.[24] To examine the expression of α9 integrin by flow cytometry analysis, we used anti-α9 integrin antibody (clone: 18R18D) which has not such an inhibitory effect.[24] As a control, normal hamster immunoglobulin G (NHG) was used.

Wounding

After shaving the dorsal hair and cleaning the exposed skin with 70% ethanol, full-thickness skin (including the panniculus carnosus) excisional wound was made on the back of 8-weeks-old female

C57BL/6 mice using 5-mm biopsy punch (Nipro, Osaka, Japan). The edges of the wound were traced onto a transparency, and the areas of open wounds were calculated using ImageJ software (Version 1.38x, NIH, Bethesda, MD, USA) as previously reported.[25] Wounds were left uncovered and harvested using 5-mm biopsy punch at 1, 3, 5, 7, 10, and 14 days after wounding.

Tissue harvesting

For histological analysis, wounds including small margin of surrounding skin were removed and bisected. Tissue was embedded in Tissue-Tek OCT compound (Sakura Finetek Japan Co., Ltd., Tokyo, Japan) and stored at -80°C. The samples were sectioned at 5μm thickness with a cryostat, air-dried for 2 hrs, and then fixed for 7 min in acetone at -20°C. Tissue sections were stored -80°C until use.

Culture of primary fibroblasts

Adult mouse subcutaneous fibroblasts were prepared from 8-week-old C57BL/6 mice. Briefly, a full thickness of the back skin was cut out by scissors, and then cut into small pieces. The skin was implanted into plastic tissue culture dishes containing TIL medium (IBL, Gunma, Japan) with 10% fetal bovine serum (PAA Laboratories GmbH, Pasching, Austria), 2mM glutamine, 100units/ml penicillin and 100μg/ml streptomycin (Sigma). After 2 weeks, proliferative cells were harvested and subcultured. The fibroblasts were used between passage 3 and 5 for experiments.

Immunohistochemistry and immunofluorescence

Tissue sections were stained with hematoxylin and eosin or used for immunohistochemistry. For immunohistochemistry, sections were blocked in 10% normal goat serum (Jackson ImmunoResearch Laboratories, Inc., West Grove, PA, USA) in phosphate-buffered saline (PBS) for 30 min at room temperature. To further block endogenous peroxidase, sections were treated with 0.3% H_2O_2 in PBS for 5 min. Sections were incubated with the primary antibody overnight at 4°C. Rat monoclonal antibodies specific for mouse CD31 (BMA Biomedicals, Augst, Switzerland), F4/80 (BioLegend, San Diego, CA, USA), mouse monoclonal antibody specific for vimentin (Sigma-Aldrich, Inc., St Louis, MO, USA), rat monoclonal antibody specific for Ki-67 (Dako Japan Inc., Tokyo, Japan) were diluted 1/400, 1/200, 1/200, 1/200 in 10% goat serum in PBS, respectively. The primary monoclonal antibody specific for α-smooth muscle actin (α-SMA) (clone 1A4, Sigma) were biotinylated by Biotin Labeling Kit – NH_2 (Dojindo Molecular Technologies, Inc, Rockville, MD, USA) and diluted at 5μg/ml. Sections were then incubated sequentially for 30 min at room temperature with a biotinylated secondary antibody, then Vectastain ABC kit (Vector Laboratories, Burlingame, CA, USA) for 30 min at room temperature. After incubation, sections were washed 3 times with PBS, developed with DAKO EnVision™+ kit/HRP (DAB) (Dako Japan Inc.), and then counterstained with hematoxylin.

For immunofluorescence, 3.0×10^4 dermal fibroblasts were plated on 0.5% gelatin pre-coated Lab-Tek II chamber slide (Thermo scientific, Rockford, IL, USA). After over night incubation,

samples were fixed in 2% paraformaldehyde followed by permeabilization with 0.1% TritonX-100. Samples were then incubated for 30 min at room temperature with either anti-vimentin (diluted 1/200) or FITC-conjugated anti-α-SMA (diluted 1/250; clone 1A4, Sigma) in TIL medium containing 10% fetal bovine serum. Samples were incubated for 30 min with FITC-conjugated anti-mouse IgM (diluted 1/100; Jackson ImmunoResearch Laboratories, Inc.) and/or rhodamine-phalloidin (diluted 1/200; Invitrogen/Molecular Probes, Carlsbad, CA, USA) in TIL medium containing 10% fetal bovine serum, then counterstained and embedded in VECTASHIELD Mounting Medium with DAPI (Vector Laboratories). For negative control, purified mouse IgM (diluted 5μg/ml; Invitrogen) was used as a substitute for primary antibody.

Image analysis and morphometry

The degree of wound healing was evaluated by using sections of wounded skin, stained with hematoxylin and eosin. The extent of wound contraction was determined by the wound width as described previously,[26] and was defined as the distance between the cut ends of the connective tissues (as indicated by arrow in Figure 7a). Granulation tissue was defined as the area that consisted of collection of vimentin-positive fibroblasts, CD31-positive newly formed blood vessels, and F4/80-positive macrophages (as shown in Figure 4a-c), as described previously.[27] Using free-hand tool of Photoshop (Version 5.5, Adobe Systems, Tokyo, Japan), the areas of granulation tissue were gated and measured using ImageJ software.

RNA isolation and real-time reverse transcriptase (RT)-PCR

Total RNA was extracted from homogenized wound tissues or isolated fibroblasts using TRIzol (Invitrogen). First strand cDNA was generated with the Transcriptor First Strand cDNA Synthesis Kit (Roche Diagnostics GmbH, Mannheim, Germany). Real-time PCR was carried out with the LightCycler FastStart DNA Master SYBR Green I Kit (Roche). Primers for α9 integrin, α4 integrin, OPN, TN-C, glyceraldehyde-3-phosphate dehydrogenase (GAPDH) were as follows, α9 integrin: 5′-AAAGGCTGCAGCTGTCCCACATGGACGAAG-3′ and 5′-TTTAGAGAGATATTCTTCACAGCCCCCAAA-3′, α4 integrin: 5’-TGGAAGCTACTTAGGCTACT-3’ and 5’-TCCCACGACTTCGGTAGTAGTAT-3’, OPN: 5’-ACGACCATGAGATTGGCAGTG-3’ and 5’-TTAGTTGACCTCAGAAGATGA-3’, TN-C: 5’-TGTGTGCTTCGAAGGCTATG-3’ and 5’-GCAGACACACTCGTTCTCCA -3’. GAPDH: 5’-ACCACAGTCCATGCCATCAC-3’ and 5’-TCCACCACCCTGTTGCTGTA-3’. Expression of real-time PCR products was normalized to GAPDH.

Western blotting

Snap-frozen wounds were homogenized in PBS with Protease Inhibitor Cocktail Tablets (Complete Mini, Roche). Dermal fibroblasts, NIH3T3 cells and murine α9 integrin transfected-NIH3T3 cells[24] were lysed in 20mM Tris-HCl (pH7.5), 150mM NaCl, 1mM EDTA, 1% TritonX-100, 2.5mM sodium pyrophosphate, 1mM β-glycerophosphate, 1mM Na_3VO_4 containing protease inhibitor

(Roche). The lysates were centrifuged at 15,000 rpm for 30 minutes to remove cell debris and then heated at 100°C for 5 min. Concentration of protein was determined using BCA Protein Assay Kit (Thermo scientific). Twenty micrograms protein lysates were separated by SDS-PAGE using 10-12% gel. Proteins were transferred onto nitrocellulose membranes. Membranes were subsequently blocked in 5% nonfat milk in 20mM Tris-HCl/136.9mM NaCl/0.1% Tween 20, followed by incubation with primary antibodies: against α-SMA (clone 1A4, Sigma), GAPDH (clone 6C5, EMD Chemicals Inc., Darmstadt, Germany) or α9 integrin (R&D systems, Minneapolis, MN, USA). After incubation with horseradish peroxides-conjugated secondary antibodies, membranes were developed using an enhanced chemiluminescence detection system (GE Healthcare UK Ltd., Buckinghamshire, England).

Flow cytometry

Fibroblasts were trypsinized, washed with PBS, blocked with rat anti-mouse CD16/CD32 (clone: 2.4G2, 5μg/ml) (BD Biosciences, San Diego, CA, USA) in FACS buffer (0.5% bovine serum albumin (BSA), 0.05% NaN_3 in PBS) on ice for 30 min, incubated with 5μg/ml biotinylated-hamster anti-mouse α9 integrin (clone:18R18D) with 500μg/ml control normal hamster immunoglobulin G (NHG) or 500μg/ml non-labeled 18R18D for 30 min on ice and then with 0.5μg/ml streptavidin-APC in FACS buffer on ice for 20 min. Labeled cells were suspended in PBS with 10μg/ml 7-Aminoactinomycin D (Sigma) for detecting dead cells, and fluorescence was

determined with a flow cytometer (FACSort, BD Biosciences).

Production of mutated forms of TN-C

The specific binding domain for α9 integrin within human TN-C exists within a third fibronectin type III repeat domain of human TN-C (R^{797}-P^{896}) and this domain also contains a binding site for RGD-recognizing integrins.[28] To study the α9 integrin-specific interaction of TN-C with fiboroblasts, a third fibronectin type III repeat domain of human TN-C (R^{797}-P^{896}) in which RGD was mutated to RAA (TN-C(RAA)),[29, 30] was generated, thus eliminating the interaction of this mutated protein with RGD-recognizing integrins and was cloned into pGEX6p-1 from cDNA derived from HT-1080 cells using a pair of primers; TN-C-5': 5'-GTTGGATCCAGGGTGACCACCACACGCTTG-3' and TN-C (RAA)-3': 5'-TCTCTCGAGTTAGGGAGCATCGAGGCCTGTTGTGAAGGTCTCTTTGGCTGGGTTGCTT GACATGGCAGCTCT -3'. pGEX plasmid was transformed to JM109 competent cells. The glutathione *S*-transferase fusion protein was purified with glutathione sepharose 4B beads, cutted off from glutathione *S*-transferase with PreScission protease (GE Healthcare). Purity and concentration of product were confirmed by SDS-PAGE followed by Coomassie Blue staining and BCA Protein Assay Kit (Thermo scientific), respectively.

Cell adhesion assay

Ninety six-well plate was coated with BSA (2.5μg/ml) or TN-C(RAA) (2.5μg/ml) in PBS for 1 hr at 37°C. Wells were blocked with 0.5% BSA in PBS for 1 hr at room temperature and then washed with PBS. Twenty thousand cells were added to each well in 200μl of serum-free TIL medium containing 0.25% BSA in the presence or absence of NHG or 55A2C (10μg/ml). Plates were incubated at 37°C. After 1 hr, the cells were washed with PBS, fixed, and stained with crystal violet. All wells were rinsed three times with water, and adherent cells were then lysed with 20% acetic acid. The resulting supernatants from each well were analyzed by an immunoreader (Thermo scientific), and the absorbance at 590 nm was measured to determine the relative number of cells adhered to wells.

Evaluation of cell migration by haptotaxis assay

To evaluate the cell migration toward an immobilized TN-C (RAA), haptotaxis assay was performed.[31] Millicell Culture Plate Insert (pore size: 8μm, Millipore, Tokyo, Japan) were used. The undersurface of the insert was coated with BSA (10μg/ml) or TN-C (RAA) (10μg/ml) in PBS for 1 hr at 37°C and blocked with 0.5% BSA in PBS for 1 hr at room temperature. Primary cultured fibroblasts were harvested and suspended in serum-free TIL medium. Then, cells were pre-treated by NHG or 55A2C (20μg/ml) in TIL medium for 20 min at 37°C, plated in the upper chamber at a density of 1.0×10^5 in 200μl of medium in the presence or absence of NHG or 55A2C (20μg/ml). After 4 hrs incubation, cells in the upper surface of the insert were removed using swab, and then

cells in the undersurface of the insert were fixed with methanol and stained with Giemsa's staining solution (Muto pure chemicals Co., LTD., Tokyo, Japan). 6 fields were counted through light microscopy and averaged for each condition studied.

Isolation of fibrocytes

Murine fibrocytes were purified from peripheral blood and cultured as previously described.[32] In brief, murine peripheral blood mononuclear cells (PBMC) were isolated from heparinized C57BL/6 mouse blood by centrifugation over Lymphosepar II (IBL) according to the manufacturer's protocol. Murine PBMC were cultured in TIL medium containing 10% fetal bovine serum and 10% mouse serum, 2mM glutamine, 100units/ml penicillin and 100μg/ml streptmycin on 24 well plate at a density of 2×10^6 cells in 1ml of medium. After 2 days, nonadherent cells were removed by gentle aspiration, and media were replaced. After 10 days, the adherent crude fibrocyte preparations were lifted using 0.05% EDTA in PBS for use of flow cytometry and RT-PCR analysis. For flow cytometry analysis, anti-CD3, B220, and CD14 antibodies were used. (CD3, CD14: BD Biosciences; B220: eBioscience (San Diego, CA, USA))

Measurement of α9 integrin and type I collagen expression in murine fibrocytes

The cell surface expression of α9 integrin on isolated fibrocytes was evaluated by flow cytometry. The expression of α9 integrin or type I collagen mRNA was evaluated by RT-PCR. For RT-PCR, to

control for any difference in quantity of total RNA among the samples, GAPDH mRNA expression was evaluated simultaneously. Total RNA was extracted from isolated fibrocyte using TRIzol (Invitrogen). First strand cDNA was generated with the Transcriptor First Strand cDNA Synthesis Kit (Roche). PCR amplification was performed using gene-specific primers and TaKaRa Ex Taq (Takara Bio, Shiga, Japan). The primers for type I collagen were as follows: Type I collagen: 5'-TTTGTGGACCTCCGGCTC-3' and 5'- AAGCACAGCACTCGCCCT-3'. (The primers for α9 integrin and GAPDH were described above.) PCR was performed with 35 cycles of 30 sec of denaturation at 94°C, 30 sec of annealing at 58°C, and 30 sec of extension at 72°C, followed by 5 min of final extension at 72°C. PCR products were separated by electrophoresis using 1.5% agarose gels and viewed under ultraviolet light after ethidium bromide staining.

Statistical analysis

Student's t-test was used for comparison of means between groups. A value of $P<0.05$ was considered significant. The error bars indicate the S.E.M.

Results

Three distinct phases of wound healing

In this study, to assess macroscopic healing process, full-thickness skin excisional wounds were made in mice using a 5-mm punch and the area of each open wound was traced at 0, 3, 5, 7, 10 and 14 days after wounding. We found that the area of open wound was significantly reduced at two time points; from day 0 to day 5 and from day 7 to day 10. However, the area of open wound remained unchanged if any from day 5 to day 7 (Figure 1). According to the previous reports, re-epithelialization and contraction of granulation tissue are important processes that can reduce the area of open wound,[1, 2] and approximate timing of these process are taken place from day 1 to day 2 and from day 4 to day 14 after wounding, respectively. In addition, granulation tissue formation occurs from day 4 to day 7 after wounding between re-epithelialization phase and wound contraction phase.[33] Therefore, we divided the process of full-thickness skin excisional wound healing into three phases; the early phase from day 0 to day 5, middle phase from day 5 to day 7, and late phase from day 7 to day 14 after wounding (Figure 1). These early, middle, and late phases are thought to correspond to the phases of re-epithelialization, formation of granulation tissue, and contraction of granulation tissue, respectively.[4, 33, 34]

Induction of α9 integrin and its ligands during the process of wound healing

Next, we examined whether the expression of α9 integrin and its ligands are induced after skin wounding. The gene expression of α9 integrin was induced on day 1 and its up-regulation maintained all the time after wounding from day 3 to day 10 (Figure 2a). We tested the expression of well known ligands for α9 integrins, OPN and TN-C. Although the both ligands are induced after wounding, the peak OPN gene expression was detected at 1 day after wounding (Figure 2c), whereas TN-C was at 5 days after wounding (Figure 2d), suggesting the distinct roles of these ECM proteins in the healing process. The gene expression of α4 integrin, which possesses a structural similarity with α9 integrin[35] was induced from day 1 to day 10 (Figure 2b). Thus, the kinetics of gene expression between α4 and α9 integrin was very similar. These results suggest that interactions of α9 or α4 integrins and their ligands take place in wounds and may be involved in the skin wound healing process.

Formation of granulation tissue is hampered by blocking α9 integrin

To examine the role of α9 integrin in the wound healing process, the blocking antibody against α9 integrin (clone: 55A2C) was given to the mice twice at 1 day prior to and at 2 days after making full-thickness skin excisional wound (Figure 3). It has been demonstrated that α9 integrin is involved in the process of re-epithelialization,[36] which occurs during the first phase of wound healing. Granulation tissue formation critically depends on the proliferation and migration of fibroblasts and angiogenesis, which occurs during the middle phase of wound healing. Granulation

tissue is defined as the area that consisted of collection of vimentin-positive fibroblasts, CD31-positive newly formed blood vessels, and F4/80-positive macrophages (Figure 4a, b, and c). Although granulation tissue was not detected at 3 days after wounding, most of wound site were occupied by granulation tissue at 10 days after wounding (Figure 4d). It should be noted that granulation tissue area was significantly reduced on day 7 in 55A2C-treated mice, as compared with NHG-treated mice (Figure 5a and b). Consistent to those data shown in Figure 5, the density of vimentin-positive fibroblasts within granulation tissue was significantly reduced on day 7 in 55A2C-treated mice (Figure 6a). Taken together, we found that the interaction of α9 integrin with its ligands plays a pivotal role for the formation of granulation tissue. Angiogenesis is necessary in wound healing to sustain the newly formed granulation tissue. Macrophage infiltration into the wound site is also important for debridement and provides a source of growth factors to repair skin.[2, 33, 34] Therefore, we examined the density of CD31-positive blood vessels and F4/80-positive macrophages within wound site at 7 days after wounding. Neither angiogenesis nor macrophage infiltration were altered in 55A2C-treated mice (Figure 6a). It should be pointed out that macrophage infiltration is evident at early phase of wound healing and macrophage may influence subsequent wound healing process.[33] Therefore, we also examined the effect of antibody treatment on the macrophage infiltration on day 3. However, we found that macrophage infiltration was not impaired by antibody treatment on day 3 (Figure 6b). We then tested whether the reduction of vimentin-positive fibroblasts is due to the inhibition of fibroblast proliferation. Therefore, we

analyzed Ki-67 positive cells within granulation tissue. In 55A2C-treated mice, although the density of fibroblasts within granulation tissue was significantly reduced, the ratio of Ki-67 positive cells against fibroblasts within granulation tissue was not altered on day 7 (Figure 6c). These data suggested that the interaction of α9 integrin with its ligands is not involved in fibroblast proliferation during the formation of granulation tissue.

Wound contraction is not affected by blocking α9 integrin

The critical process in the late phase of wound healing is the contraction of granulation tissue, which is reflected by connective tissue wound width. Wound width is expressed by the distance between the cut ends of the connective tissues (as indicated by closed arrows in Figure 7a). Kinetics of wound contraction was depicted as representative histology in Figure 7b. As summarized in Figure 7c, wound width is markedly reduced between day 7 and day 10, indicating that wound contraction occurs from day 7 to day 10, which is consistent with our data that open wound area is significantly reduced at late phase (Figure 1). The contraction force is provided by the differentiated myofibroblasts within granulation tissue.[37] Myofibroblasts were marked as α-SMA-positive cells as shown in Figure 7d. The α-SMA staining was peaked on day 7 and significantly reduced at 14 days after wounding, again confirming that wound contraction occurs from day 7 to day 10 (Figure 7d). However, α-SMA-positive area did not differ between NHG and 55A2C-treated mice at 7 and 10 days after wounding (Figure 7d). Furthermore, western blot

analysis of wounded tissues showed that the expression of α-SMA protein did not differ between NHG and 55A2C-treated mice at 7 and 10 days after wounding (Figure 7e and f). Consistent to those findings, wound width was not significantly different between NHG and 55A2C-treated mice at each time point after wounding (Figure 7c). Thus, our data demonstrated that the interaction of α9 integrin and its ligands is not critically involved in the process of wound contraction.

Adhesion and migration of fibroblasts are impaired by blocking α9 integrin

We then analyzed the molecular basis for the reduction of wound area (Fig 5a, b) and fibroblast density (Fig 6a) in granulation tissue in 55A2C-treated mice. We found that fibroblasts isolated from wound site at each time point expressed α9 integrin (Figure 8a). Next, dermal fibroblasts obtained from uninjured subcutaneous tissue of adult mice were cultured. These cells were F4/80^{-} cells (data not shown[24]) and were positive for vimentin and negative for α-SMA and exhibited morphological features of fibroblasts (Figure 8b[24]). Importantly, dermal fibroblasts expressed α9 integrin as detected by flow cytometry and western blot analysis (Figure 8c and d, respectively). α9 integrin, expressed by those fibroblasts is functional since cells were able to bind to its ligand, TN-C, and this adhesion was specifically inhibited by 55A2C (Figure 8e). In addition, we found that TN-C induced significant migration of dermal fibroblasts and this migration was specifically inhibited by 55A2C (Figure 8f). We also found that the interaction between fibroblasts and TN-C did not induce cell proliferation and the fibroblast proliferation was not altered by 55A2C (data not

shown). Taken together, these data suggest that α9 integrin is involved in granulation tissue formation via regulating fibroblast migration and adhesion.

α9 integrin was not expressed on circulating fibrocyte

Recent study has shown that there is a population of circulating fibrocytes in peripheral blood and those fibrocytes are bone marrow-derived mesenchymal progenitors, which is believed to contribute to wound healing.[38, 39] Therefore, we examined whether α9 integrin is expressed on murine fibrocytes that were purified from peripheral blood as previously described.[32] Murine PBMC contained less than 14% of non-T cells, non-B cells and non-monocytes (Figure 9a). PBMC were then cultured in vitro for 12 days as described in materials and methods section and crude fibrocytes population was obtained. This population contained approximately 73% of non-T cells, non B-cells and non-monocytes (Figure 9b). We could not detect any expression of α9 integrin in fibrocytes by both flow cytometric analysis (Figure 9c) and RT-PCR analysis (Figure 9d). Nevertheless, control fibroblasts expressed both α9 integrin and type I collagen genes. However, fibrocytes expressed only type I collagen gene as expected, but not α9 integrin.

Discussion

Wound healing process can be divided into three distinct phases, including 1) re-epithelialization, induced by keratinocyte migration and proliferation, judged by epithelial gap and keratinocyte area, 2) formation of granulation tissue, evidenced by dense vimentin positive dermal fibroblasts and CD31 positive blood vessels, and 3) contraction of granulation tissue, facilitated by differentiation of dermal fibroblasts into myofibroblasts. Previous reports showed that the interaction of various integrins with ECM proteins has critical roles in distinct phases of skin wound healing process via the modulation of neutrophil infiltration,[40] re-epithlilazation,[8, 41] fibroblast migration,[42] angiogenesis[6, 7] and myofibroblast differentiation.[43, 44] Migrating keratinocytes at the wound edge express several intergins, including collagen receptor α2β1, laminin receptors α3β1 and α6β4, fibronectin receptors αvβ6 and α5β1, and vitronectin receptor αvβ5.[41, 45] These integrins play a critical role in keratinocyte migration and proliferation, thus re-epthelialization process. α9β1 integrin is found to be expressed on migrating keratinocytes.[20] It has been shown that the proliferation of keratinocytes was suppressed during skin wound healing under the condition in which epithelial cell lacks α9 integrin. The reduced keratinocyte proliferation observed in those mice negatively impacts on wound healing, resulting in a thinner migrating epithelium, thus demonstrating that α9 integrin is crucial for efficient and proper re-epithelialization during cutaneous wound healing.[36] However, the role of α9 integrin at various healing phases of

full-thickness wounds in mice still remains to be elucidated. Therefore, we examined the role of α9 integrin during the course of wound healing using anti-mouse α9 integrin antibody (clone: 55A2C).

α9 integrin is involved in the formation of granulation tissue

Around 4 days after injury, granulation tissues, which are composed of macrophages, fibroblasts, newly blood vessels and collagens, begin to be formed in wound site. Macrophages are thought to be important for debridement of dead cells and provide a source of growth factors to cause the proliferation of endothelial cells or fibroblasts.[2, 33, 34] Fibroblasts are the most important mesenchymal cells involved in wound healing and main source of ECM deposition and reorganization within the wound bed. Among several ECM proteins, collagen produced by fibroblasts causes fibrinogenesis and strengthens the wounds. Angiogenesis is necessary in wound healing to sustain the newly formed granulation tissue. Thus, it has been thought that various types of cells in granulation tissue affect the quality of wound healing processes. Dermal fibroblasts strongly expressed α9 integrin and dermal fibroblast migration was significantly blocked by 55A2C *in vitro*, indicating that α9 integrin is involved in fibroblast movement (Figure 8). Further, it is believed that dermal fibroblasts have a critical role in the formation of granulation tissue.[33, 34] Therefore, we measured the granulation tissue area to evaluate whether administration of 55A2C affects the granulation tissue formation. As expected, granulation tissue area was reduced in 55A2C-treated mice (Figure 5a and b). Moreover, the density of fibroblasts within granulation

tissue was significantly reduced on day 7 in 55A2C-treated mice (Figure 6a). In wound healing process, the expression of not only α9 integrin but also OPN and TN-C was highly up-regulated (Figure 2). In addition, it has been also reported that EDA/EIIIA segment of fibronectin which is a ligand for α9β1 integrin is expressed during the granulation tissue phase of wound healing.[19-22] It should be pointed out that α9 integrin is not involved in fibroblast proliferation (Figure 6c). Taken together, these results and reports suggest that the interaction of α9 integrin on the dermal fibroblasts with its ligands such as OPN, TN-C and EDA/EIIIA segment of fibronectin is involved in the migration of dermal fibroblasts into wound site, thereby facilitating the formation of granulation tissue.

It should be pointed out that the origin of α9 integrin-positive fibroblasts found in wounded skin is of still controversial. It is reasonable to assume that fibroblasts migrate into the wounded site from surrounding skin tissues. It is possible that both migrated dermal fibroblasts from the surrounding skin tissues and residual resident dermal fibroblasts contribute to the α9 integrin-positive fibroblasts found in wounded skin. In addition, recent study has shown that there is a population of circulating fibrocytes in peripheral blood and those fibrocytes are bone marrow-derived mesenchymal progenitors, which is believed to contribute to wound healing.[38, 39] Therefore, we examined whether α9 integrin is expressed on murine fibrocytes that were purified from peripheral blood. We could not detect any expression of α9 integin on fibrocytes, suggesting that the contribution of circulating fibrocytes to the wound healing process is α9 integrin

independent (Figure 9). It is also possible that fibrocytes initiate α9 expression as - or subsequent to - their entry into the wound bed.

Other important issue that should be discussed here is the contribution of α9 integrin to the angiogenesis. It is known that granulation tissue consists of not only dense collection of vimentin-positive fibroblasts but also CD31-positive blood vessels. Mice lacking α9 integrin dies due to the deficient development of major lymph vessels, thoracic duct,[23] raising the possibility that α9 integrin is also involved in angiogenesis. However, we found that the density of CD31-positive blood vessels within granulation tissues was not altered in 55A2C-treated mice (Figure 6a). In this regard, it should be noted that fibronectin and vitronectin receptors, such as αvβ3 and α5β1 integrins, were involved in the angiogenesis in skin wound healing models.[6, 7, 46, 47]

α9 integrin is not involved in wound contraction

The contraction of granulation tissue, which is the late phase of wound healing, is mainly mediated by the differentiated myofibroblasts.[48] Wound contraction and the area of α-SMA-positive cells in wounded tissue is not affected by blocking α9 integrin, suggesting that α9 integrin is not involved in myofibroblast differentiation (Figure 7d). We also found that TGF-β-induced gel-contraction is not affected by 55A2C, supporting the idea that the differentiation of myofibroblast is independent of the interaction between α9 integrin and ECM proteins (data not shown).

Although the formation of granulation tissue is impaired, the contraction of granulation tissue as

well as the area of open wound is unchanged by blocking α9 integrin. It is possible that the number of fibroblasts in granulation tissue of 55A2C-treated mice is sufficient for making wound contraction since the preventive effect of 55A2C on the formation of granulation tissues is partial (Figure 5a). Furthermore, the other integrins such as αv and α5β1 which mainly involved in the fibroblast migration or myofibroblast differentiation may compensate for the function of α9 integrin.

In summary, we found that 1) mRNA of α9 integrin was up-regulated in wounded skin. 2) Dermal fibroblasts expressed α9 integrin and dermal fibroblast migration was blocked by blocking the interaction of α9 integrin with its ligands. 3) In full-thickness excisional wound model, contraction of granulation tissue was not affected by blocking the interaction of α9 integrin with its ligands. 4) Whereas, formation of granulation tissue was hampered by blocking the interaction of α9 integrin with its ligands. These results provide the evidence that α9 integrin has an important role in the formation of granulation tissue via regulating fibroblast migration during skin wound healing.

References

1. Martin P. Wound healing--aiming for perfect skin regeneration. *Science* 1997;276:75-81.
2. Singer AJ, Clark RA. Cutaneous wound healing. *N Engl J Med* 1999;341:738-746.
3. Raghow R. The role of extracellular matrix in postinflammatory wound healing and fibrosis. *Faseb J* 1994;8:823-831.
4. Midwood KS, Williams LV, Schwarzbauer JE. Tissue repair and the dynamics of the extracellular matrix. *Int J Biochem Cell Biol* 2004;36:1031-1037.
5. Werner S, Grose R. Regulation of wound healing by growth factors and cytokines. *Physiol Rev* 2003;83:835-870.
6. Mahabeleshwar GH, Feng W, Phillips DR, et al. Integrin signaling is critical for pathological angiogenesis. *J Exp Med* 2006;203:2495-2507.
7. Jang YC, Arumugam S, Gibran NS, et al. Role of alpha(v) integrins and angiogenesis during wound repair. *Wound Repair Regen* 1999;7:375-380.
8. Santoro MM, Gaudino G. Cellular and molecular facets of keratinocyte reepithelization during wound healing. *Exp Cell Res* 2005;304:274-286.
9. O'Toole EA. Extracellular matrix and keratinocyte migration. *Clin Exp Dermatol* 2001;26:525-530.
10. Bornstein P, Sage EH. Matricellular proteins: extracellular modulators of cell function. *Curr Opin Cell Biol* 2002;14:608-616.
11. Kyriakides TR, Bornstein P. Matricellular proteins as modulators of wound healing and the foreign body response. *Thromb Haemost* 2003;90:986-992.
12. Kyriakides TR, Tam JW, Bornstein P. Accelerated wound healing in mice with a disruption of the thrombospondin 2 gene. *J Invest Dermatol* 1999;113:782-787.
13. Forsberg E, Hirsch E, Frohlich L, et al. Skin wounds and severed nerves heal normally in mice lacking tenascin-C. *Proc Natl Acad Sci U S A* 1996;93:6594-6599.
14. Liaw L, Birk DE, Ballas CB, et al. Altered wound healing in mice lacking a functional osteopontin gene (spp1). *J Clin Invest* 1998;101:1468-1478.
15. Puolakkainen PA, Bradshaw AD, Brekken RA, et al. SPARC-thrombospondin-2-double-null mice exhibit enhanced cutaneous wound healing and increased fibrovascular invasion of subcutaneous polyvinyl alcohol sponges. *J Histochem Cytochem* 2005;53:571-581.
16. Agah A, Kyriakides TR, Lawler J, et al. The lack of thrombospondin-1 (TSP1) dictates the course of wound healing in double-TSP1/TSP2-null mice. *Am J Pathol* 2002;161:831-839.
17. Yokosaki Y, Palmer EL, Prieto AL, et al. The integrin alpha 9 beta 1 mediates cell attachment to a non-RGD site in the third fibronectin type III repeat of tenascin. *J Biol Chem* 1994;269:26691-26696.
18. Yokosaki Y, Matsuura N, Sasaki T, et al. The integrin alpha(9)beta(1) binds to a novel recognition sequence (SVVYGLR) in the thrombin-cleaved amino-terminal fragment of osteopontin. *J Biol Chem* 1999;274:36328-36334.
19. Muro AF, Chauhan AK, Gajovic S, et al. Regulated splicing of the fibronectin EDA exon is

essential for proper skin wound healing and normal lifespan. *J Cell Biol* 2003;162:149-160.

20. Singh P, Reimer CL, Peters JH, et al. The spatial and temporal expression patterns of integrin alpha9beta1 and one of its ligands, the EIIIA segment of fibronectin, in cutaneous wound healing. *J Invest Dermatol* 2004;123:1176-1181.

21. Liao YF, Gotwals PJ, Koteliansky VE, et al. The EIIIA segment of fibronectin is a ligand for integrins alpha 9beta 1 and alpha 4beta 1 providing a novel mechanism for regulating cell adhesion by alternative spliing. *J Biol Chem* 2002;277:14467-14474.

22. Shinde AV, Bystroff C, Wang C, et al. Identification of the peptide sequences within the EIIIA (EDA) segment of fibronectin that mediate integrin alpha9beta1-dependent cellular activities. *J Biol Chem* 2008;283:2858-2870.

23. Huang XZ, Wu JF, Ferrando R, et al. Fatal bilateral chylothorax in mice lacking the integrin alpha9beta1. *Mol Cell Biol* 2000;20:5208-5215.

24. Kanayama M, Kurotaki D, Morimoto J, et al. Alpha9 integrin and its ligands constitute critical joint microenvironments for development of autoimmune arthritis. *J Immunol* 2009;182:8015-8025.

25. Yahata Y, Shirakata Y, Tokumaru S, et al. A novel function of angiotensin II in skin wound healing. Induction of fibroblast and keratinocyte migration by angiotensin II via heparin-binding epidermal growth factor (EGF)-like growth factor-mediated EGF receptor transactivation. *J Biol Chem* 2006;281:13209-13216.

26. Mori R, Shaw TJ, Martin P. Molecular mechanisms linking wound inflammation and fibrosis: knockdown of osteopontin leads to rapid repair and reduced scarring. *J Exp Med* 2008;205:43-51.

27. Yukami T, Hasegawa M, Matsushita Y, et al. Endothelial selectins regulate skin wound healing in cooperation with L-selectin and ICAM-1. *J Leukoc Biol* 2007;82:519-531.

28. Bourdon MA, Ruoslahti E. Tenascin mediates cell attachment through an RGD-dependent receptor. *J Cell Biol* 1989;108:1149-1155.

29. Marcinkiewicz C, Taooka Y, Yokosaki Y, et al. Inhibitory effects of MLDG-containing heterodimeric disintegrins reveal distinct structural requirements for interaction of the integrin alpha 9beta 1 with VCAM-1, tenascin-C, and osteopontin. *J Biol Chem* 2000;275:31930-31937.

30. Taooka Y, Chen J, Yednock T, et al. The integrin alpha9beta1 mediates adhesion to activated endothelial cells and transendothelial neutrophil migration through interaction with vascular cell adhesion molecule-1. *J Cell Biol* 1999;145:413-420.

31. Wu RX, Laser M, Han H, et al. Fibroblast migration after myocardial infarction is regulated by transient SPARC expression. *J Mol Med* 2006;84:241-252.

32. Abe R, Donnelly SC, Peng T, et al. Peripheral blood fibrocytes: differentiation pathway and migration to wound sites. *J Immunol* 2001;166:7556-7562.

33. Baum CL, Arpey CJ. Normal cutaneous wound healing: clinical correlation with cellular and molecular events. *Dermatol Surg* 2005;31:674-686; discussion 686.

34. Li J, Chen J, Kirsner R. Pathophysiology of acute wound healing. *Clin Dermatol* 2007;25:9-18.

35. Palmer EL, Ruegg C, Ferrando R, et al. Sequence and tissue distribution of the integrin alpha 9 subunit, a novel partner of beta 1 that is widely distributed in epithelia and muscle. *J Cell Biol*

1993;123:1289-1297.

36. Singh P, Chen C, Pal-Ghosh S, et al. Loss of integrin alpha9beta1 results in defects in proliferation, causing poor re-epithelialization during cutaneous wound healing. *J Invest Dermatol* 2009;129:217-228.

37. Grinnell F. Fibroblasts, myofibroblasts, and wound contraction. *J Cell Biol* 1994;124:401-404.

38. Bellini A, Mattoli S. The role of the fibrocyte, a bone marrow-derived mesenchymal progenitor, in reactive and reparative fibroses. *Lab Invest* 2007;87:858-870.

39. Ishii G, Sangai T, Sugiyama K, et al. In vivo characterization of bone marrow-derived fibroblasts recruited into fibrotic lesions. *Stem Cells* 2005;23:699-706.

40. Peters T, Sindrilaru A, Hinz B, et al. Wound-healing defect of CD18(-/-) mice due to a decrease in TGF-beta1 and myofibroblast differentiation. *Embo J* 2005;24:3400-3410.

41. Watt FM. Role of integrins in regulating epidermal adhesion, growth and differentiation. *Embo J* 2002;21:3919-3926.

42. Greiling D, Clark RA. Fibronectin provides a conduit for fibroblast transmigration from collagenous stroma into fibrin clot provisional matrix. *J Cell Sci* 1997;110 (Pt 7):861-870.

43. Lygoe KA, Norman JT, Marshall JF, et al. AlphaV integrins play an important role in myofibroblast differentiation. *Wound Repair Regen* 2004;12:461-470.

44. Lygoe KA, Wall I, Stephens P, et al. Role of vitronectin and fibronectin receptors in oral mucosal and dermal myofibroblast differentiation. *Biol Cell* 2007;99:601-614.

45. Larjava H, Salo T, Haapasalmi K, et al. Expression of integrins and basement membrane components by wound keratinocytes. *J Clin Invest* 1993;92:1425-1435.

46. Yang JT, Rayburn H, Hynes RO. Embryonic mesodermal defects in alpha 5 integrin-deficient mice. *Development* 1993;119:1093-1105.

47. Kim S, Bell K, Mousa SA, et al. Regulation of angiogenesis in vivo by ligation of integrin alpha5beta1 with the central cell-binding domain of fibronectin. *Am J Pathol* 2000;156:1345-1362.

48. Gabbiani G. The myofibroblast in wound healing and fibrocontractive diseases. *J Pathol* 2003;200:500-503.

Titles and legends to figures

Figure 1. Kinetics of wound closure. Wound closure was measured at the indicated time points after wounding, and the edges of the wound were traced onto a transparency, and the areas of open wounds were calculated. The area of open wound was significantly reduced at two time points; during the early phase from day 0 to day 5 and middle-late phase from day 7 to 10. For each time point at least 6 wounds were measured. * : $p < 0.05$.

Figure 2. Induction of gene expression of α9 integrin and its ligands. The gene expression of α9 integrin (**a**), α4 integrin (**b**), OPN (**c**) and TN-C (**d**) in wound site at the indicated time points post wounding. For each time point at least 4 wounds were examined. N : normal skin. * : $p < 0.05$. ** : $p < 0.005$.

Figure 3. Treatment protocol of full-thickness skin excisional wound model. Mice were treated by administration of the blocking antibody against α9 integrin. NHG or 55A2C was given to the mouse, at 1 day prior to and at 2 days after making wounds.

Figure 4. Evaluation of granulation tissue. Granulation tissue (Gt) was defined by dense collection of fibroblasts (**a**) and vimentin-positive cells (**b**) and formation of CD31-positive blood vessels (**c**). (**d**) Kinetics of granulation tissue formation. Tissues were obtained at indicated time points and

were marked as Gt according to the definition described above. Solid lines encompass granulation tissue. Scale bars in **c**, 500μm (low magnification) and 200μm (high magnification); in **d**, 200μm. (Color images in this figure were mentioned in Supplemental Material 1.)

Figure 5. Formation of granulation tissue is hampered by administration of 55A2C. (**a**) Area of granulation tissue was measured. Granulation tissues were obtained from mice treated with NHG (closed bars) or 55A2C (open bars) on day 7. (**b**) Representative histology used for evaluation in (**a**). Solid lines encompass granulation tissue (Gt). Nine wounds were measured per each group. Scale bar in **b**, 500μm. * : $p < 0.05$. ** : $p < 0.005$.

Figure 6. Dermal fibroblast density was significantly decreased in 55A2C-treated wounds. (**a**) Representative histology from mice treated with NHG (left panels; closed bars) or 55A2C (right panels; open bars) on day 7. Numbers of dermal fibroblasts, CD31 positive blood vessels and F4/80 positive macrophages were counted in granulation tissue. (**b**) Numbers of macrophages were quantified for NHG- (closed bars) and 55A2C-treated wounds (open bars) on day 3. (**c**) Ratio of Ki-67 positive proliferative cells against fibroblasts within NHG- (closed bars) and 55A2C-treated (open bars) granulation tissue on day 7. Six to nine wounds were measured per each group, and 6 fields were counted through light microscopy for each section. Scale bars in **a**, **b**, and **c**, 100μm. * : $p < 0.05$. (Color images in this figure were mentioned in Supplemental Material 2.)

Figure 7. Histological evaluation of wounded skin tissues in 55A2C-treated mice. (**a**) Arrowheads represent the leading edges of migrating epithelial lips and arrows indicate the cut ends of skin connective tissue. A distance between two cut ends represents wound width. (**c**) Quantification of wound widths on day 3, 5, 7, 10 and 14. (closed bars): NHG, (open bars): 55A2C. Sections of wounded skin from mice treated with NHG (left panels) and 55A2C (right panels) were stained with hematoxylin and eosin (**b**) or anti-α-SMA (**d**) to evaluate wound width or myofibroblast differentiation, respectively at indicated time points. (**e**) Expression of α-SMA was examined on day 3, 7 and 10 by western blotting. (**f**) Semiquantitative analysis of western blotting on day 7 and 10. For each time point at least 6 wounds (**c**) or 5 wounds (**e, f**) were examined per each group. Scale bars in **b**, 1mm; in **d**, 500μm. * : $p < 0.05$.

Figure 8. α9 integrin mediated cell adhesion and migration of dermal fibroblasts. (**a**) Flow cytometry analysis of α9 integrin expression by fibroblasts derived from wound site. (**b**) Dermal fibroblasts obtained from subcutaneous tissue were stained for control Ab (left), anti-vimentin (middle) and anti-αSMA (right) (Green). Nuclei and cytoskeletal actin were visualized by DAPI (Blue) and phalloidin (Red) staining, respectively. (**c**) Dermal fibroblasts used in (**b**) were tested for the cell surface expression of α9 integrin by flow cytometry. (**d**) α9 integrin expression was also tested by western blot analaysis. Two lots of cultured dermal fibroblasts (#1 and #2) were used. NIH3T3 fibroblasts served for negative control and NIH3T3 cells, transfected with murine α9

integrin (α9/NIH) served for positive control. (**e**) Adhesion of dermal fibroblasts to ligands for α9 integrin. The adhesion of fibroblasts to the plates coated with 2.5μg/ml TN-C (RAA) or 2.5μg/ml BSA was tested in the presence of 10μg/ml NHG or 55A2C. (**f**) Dermal fibroblasts migration was assessed in a Millicell Culture Plate Insert (8.0μm). Cells were added to the upper chamber of the membrane coated with 10μg/ml BSA or TN-C (RAA). The migration of fibroblasts to TN-C (RAA) was tested in the presence of 20 μg/ml NHG or 55A2C. Six fields were counted through light microscopy and averaged for each group. Each value represents the mean ± S.E.M. of three experiments. Scale bars in **b**, 50μm. * : $p < 0.05$.

Figure 9. Expression of α9 integrin on fibrocytes. Murine peripheral blood mononuclear cells (PBMC) (**a**) and *in vitro* cultured fibrocyte enriched population (**b**) were stained with anti-CD3 (T cells), anti-B220 (B cells) and anti-CD14 (monocytes) antibodies. Note that non-T cells , non-B cells, and non-monocytes within PBMC (**a**) and fibrocyte enriched population (**b**) were 14% and 73%, respectively. (**c**) $CD3^-/B220^-/CD14^-$ cells in (**b**) were stained with anti-α9 integrin antibody. Note that fibrocyte enriched population was negative for α9 integrin expression. (**d**) Gene expression of fibrocyte marker, type I collagen, and α9 integrin in dermal fibroblasts and fibrocytes derived from PBMC. The RT-PCR for GAPDH was used as a control.

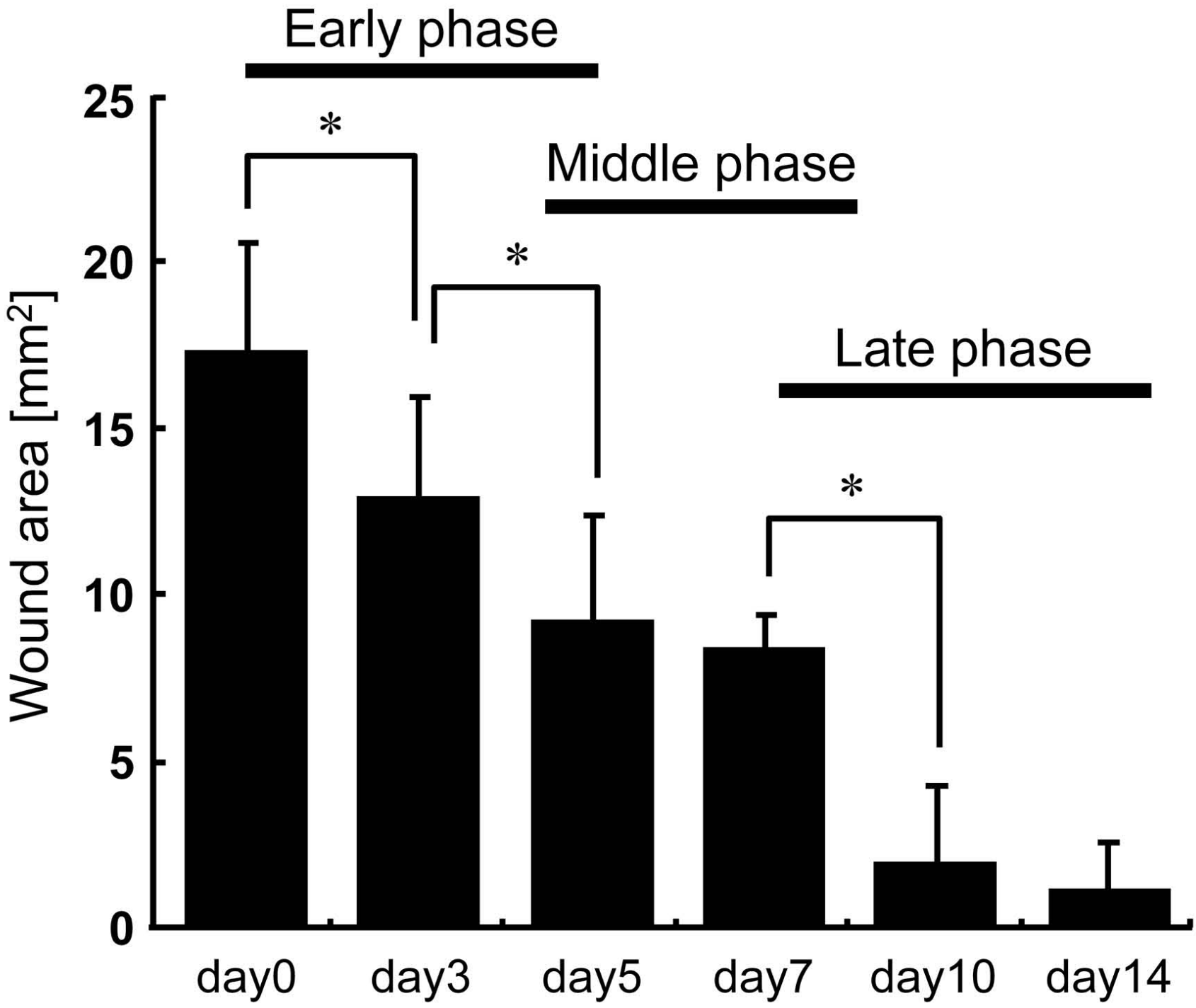
Early phase
Middle phase
Late phase
Wound area [mm2]
25
20
15
10
5
0
*
*
*
day0
day3
day5
day7
day10
day14

Figure 1

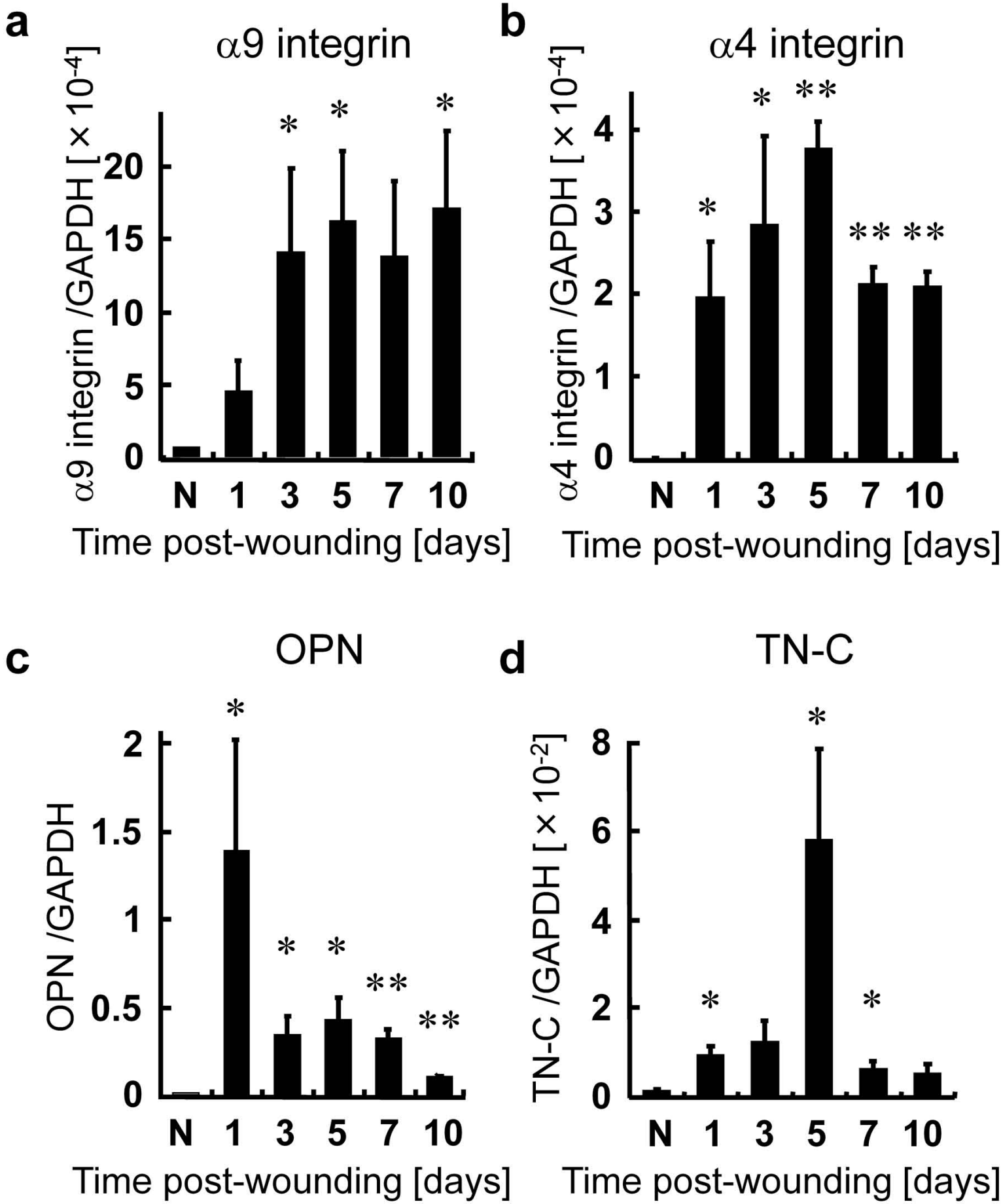
a
α9 integrin
α9 integrin /GAPDH [× 10-4]
0
5
10
15
20
N 1 3 5 7 10
Time post-wounding [days]
b
α4 integrin
α4 integrin /GAPDH [× 10-4]
0
1
2
3
4
N 1 3 5 7 10
Time post-wounding [days]
c
OPN
OPN /GAPDH
0
0.5
1
1.5
2
N 1 3 5 7 10
Time post-wounding [days]
d
TN-C
TN-C /GAPDH [× 10-2]
0
2
4
6
8
N 1 3 5 7 10
Time post-wounding [days]

Figure 2

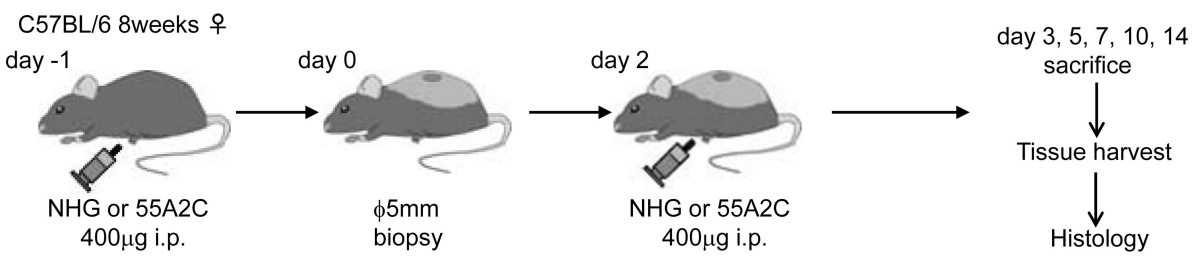
C57BL/6 8weeks ♀
day -1
NHG or 55A2C
400μg i.p.
day 0
ϕ5mm
biopsy
day 2
NHG or 55A2C
400μg i.p.
day 3, 5, 7, 10, 14
sacrifice
Tissue harvest
Histology

Figure 3

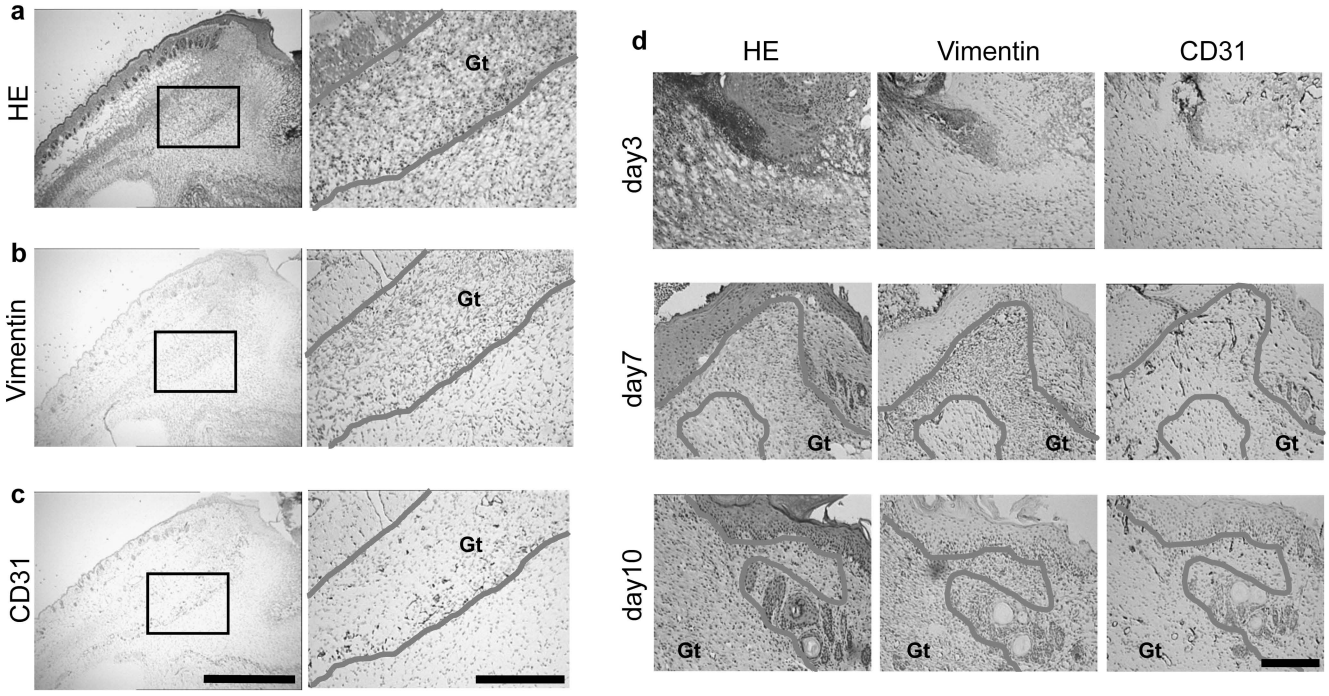
a
HE
Gt
b
Vimentin
Gt
c
CD31
Gt
d
HE
Vimentin
CD31
day3
day7
day10
Gt
Gt
Gt
Gt
Gt
Gt
Gt
Gt
Gt

Figure 4

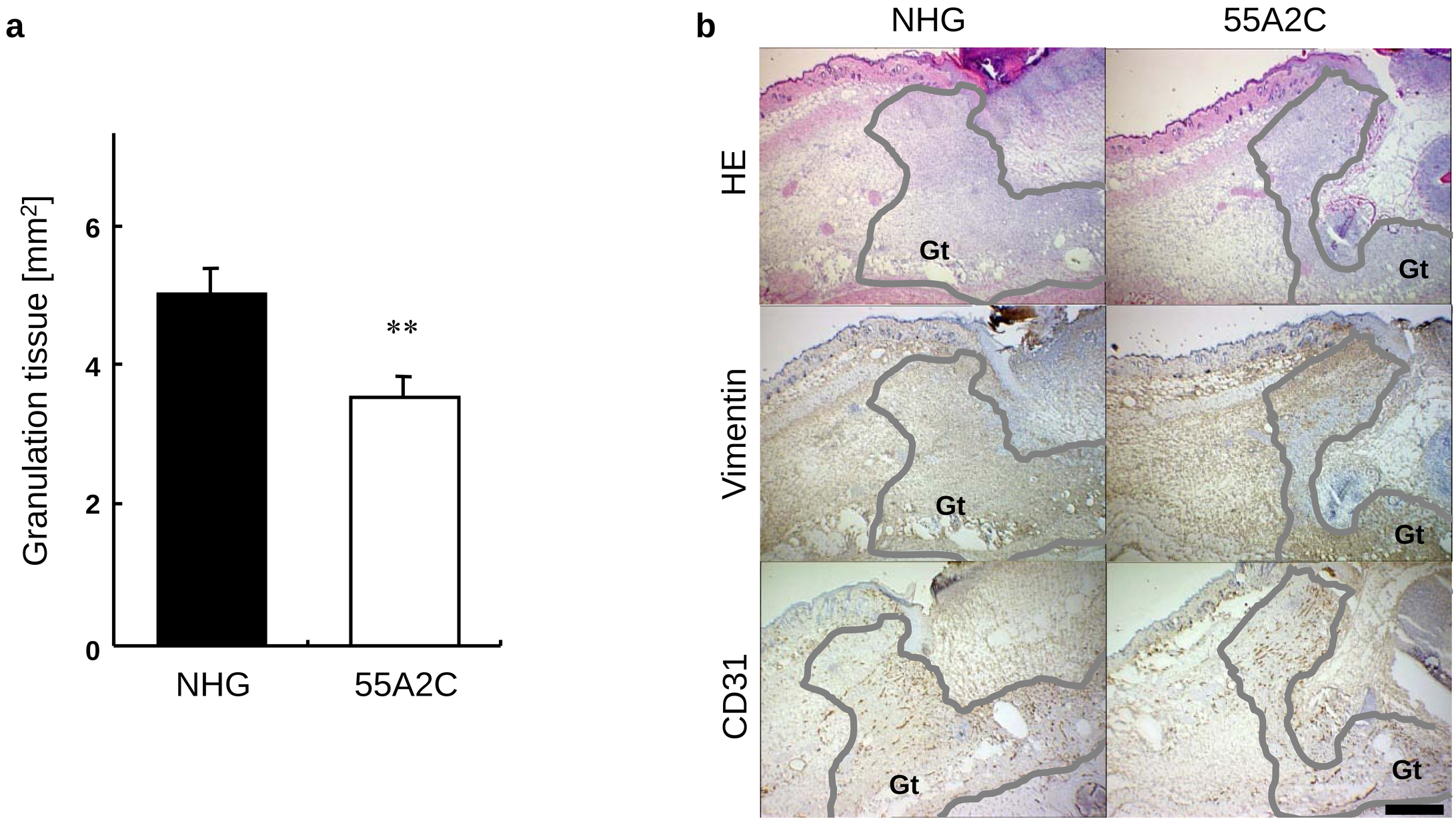
a
Granulation tissue [mm2]
6
4
2
0
**
NHG
55A2C
b
NHG
55A2C
HE
Vimentin
CD31
Gt
Gt
Gt
Gt
Gt
Gt

Figure 5

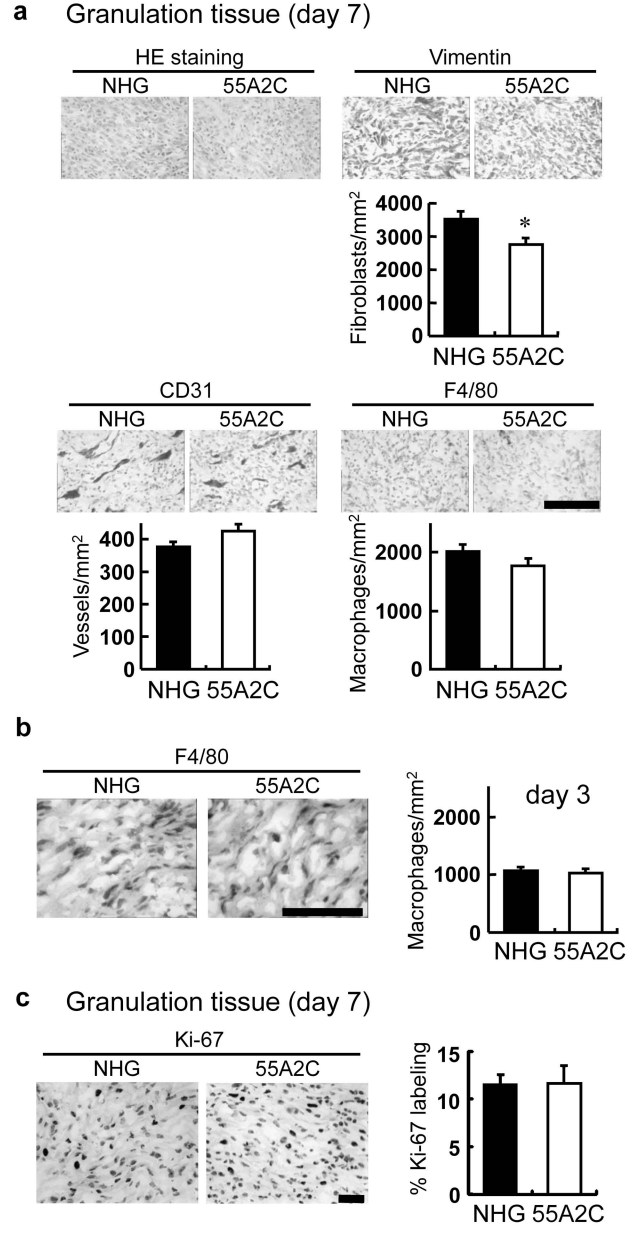
a
Granulation tissue (day 7)
HE staining
NHG
55A2C
Vimentin
NHG
55A2C
Fibroblasts/mm2
4000
3000
2000
1000
0
*
NHG 55A2C
CD31
NHG
55A2C
F4/80
NHG
55A2C
Vessels/mm2
400
300
200
100
0
NHG 55A2C
Macrophages/mm2
2000
1000
0
NHG 55A2C
b
F4/80
NHG
55A2C
day 3
Macrophages/mm2
2000
1000
0
NHG 55A2C
c
Granulation tissue (day 7)
Ki-67
NHG
55A2C
% Ki-67 labeling
15
10
5
0
NHG 55A2C

Figure 6

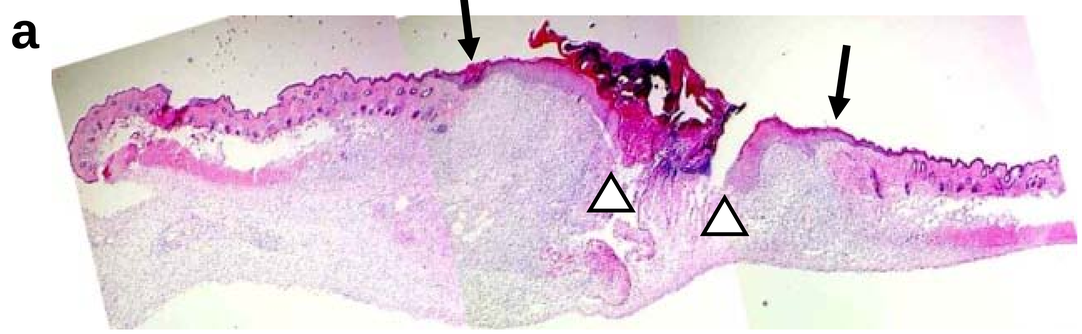
a

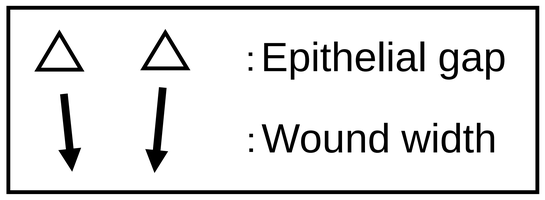
: Epithelial gap
: Wound width

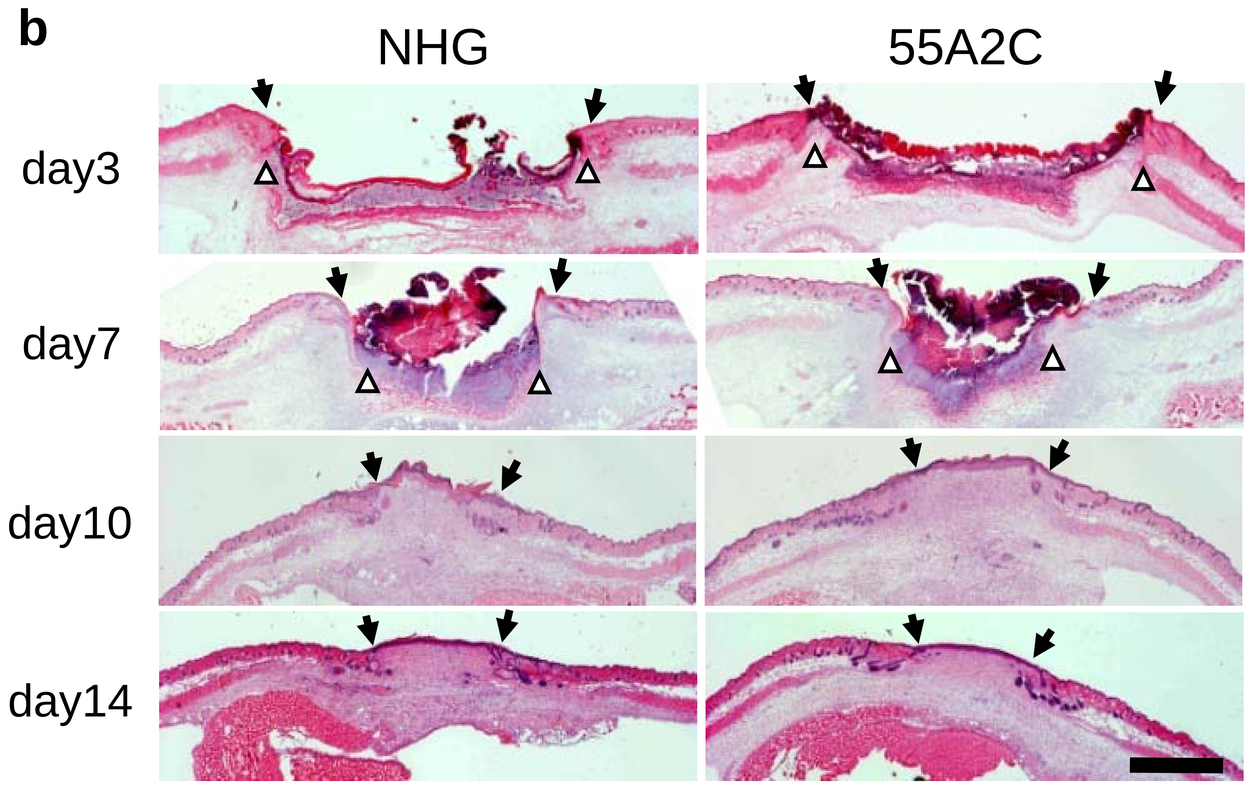
b
NHG
55A2C
day3
day7
day10
day14

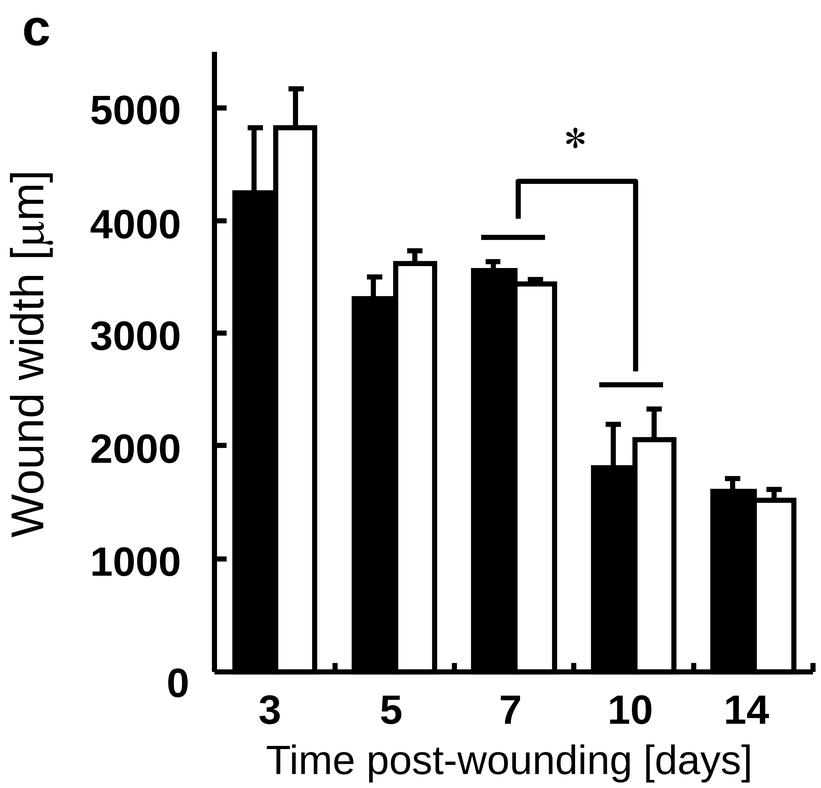
c
Wound width [μm]
5000
4000
3000
2000
1000
0
*
3
5
7
10
14
Time post-wounding [days]

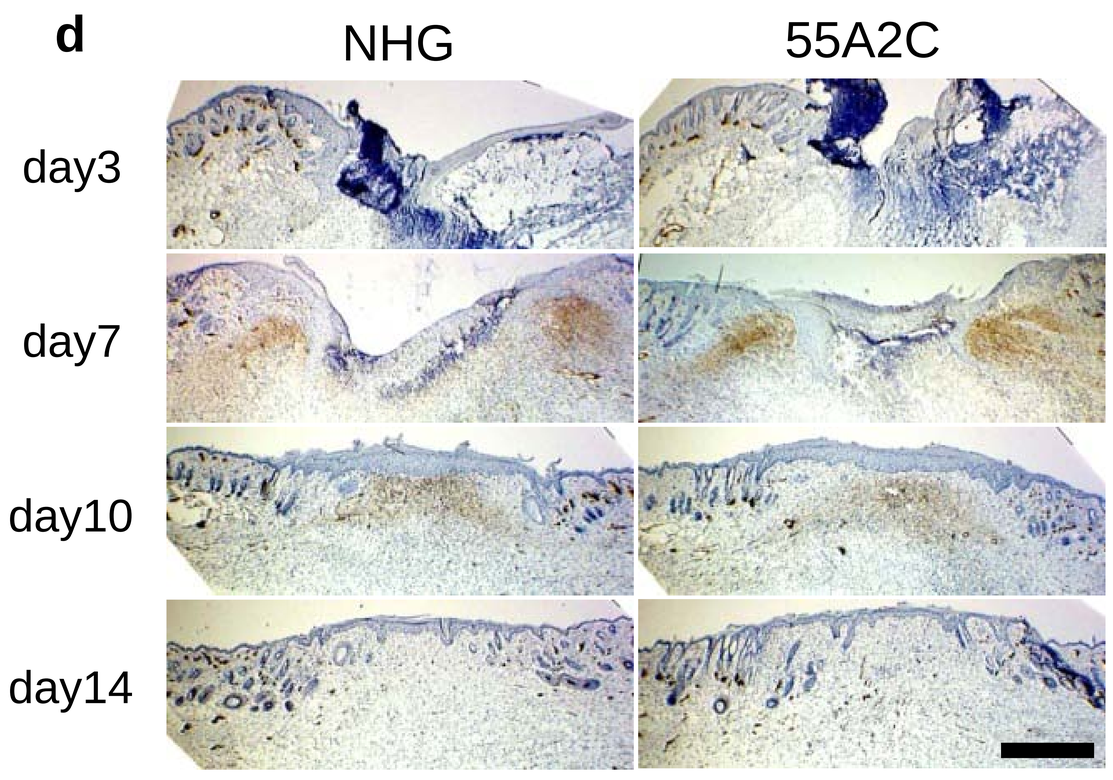
d
NHG
55A2C
day3
day7
day10
day14

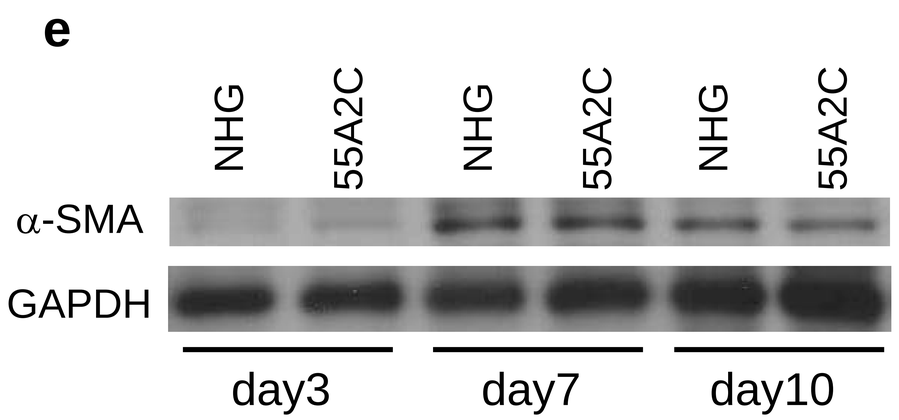
e
NHG
55A2C
NHG
55A2C
NHG
55A2C
α-SMA
GAPDH
day3
day7
day10

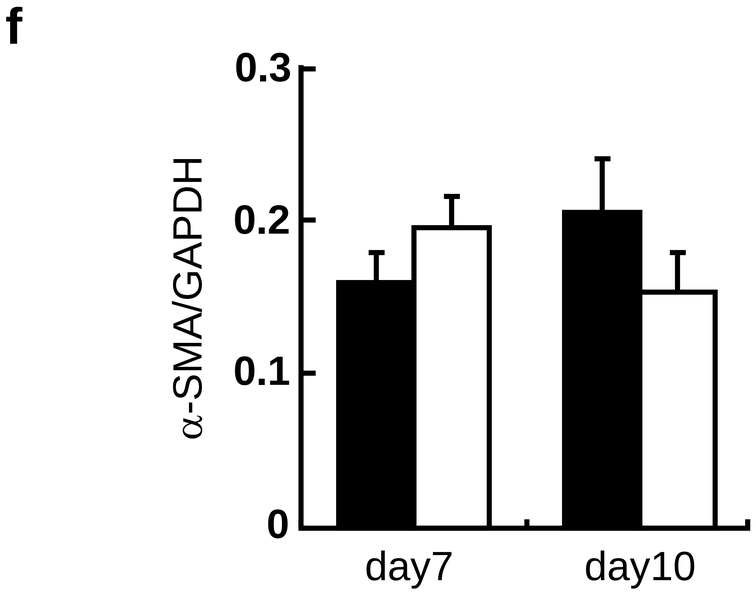
f
α-SMA/GAPDH
0.3
0.2
0.1
0
day7
day10

Figure 7

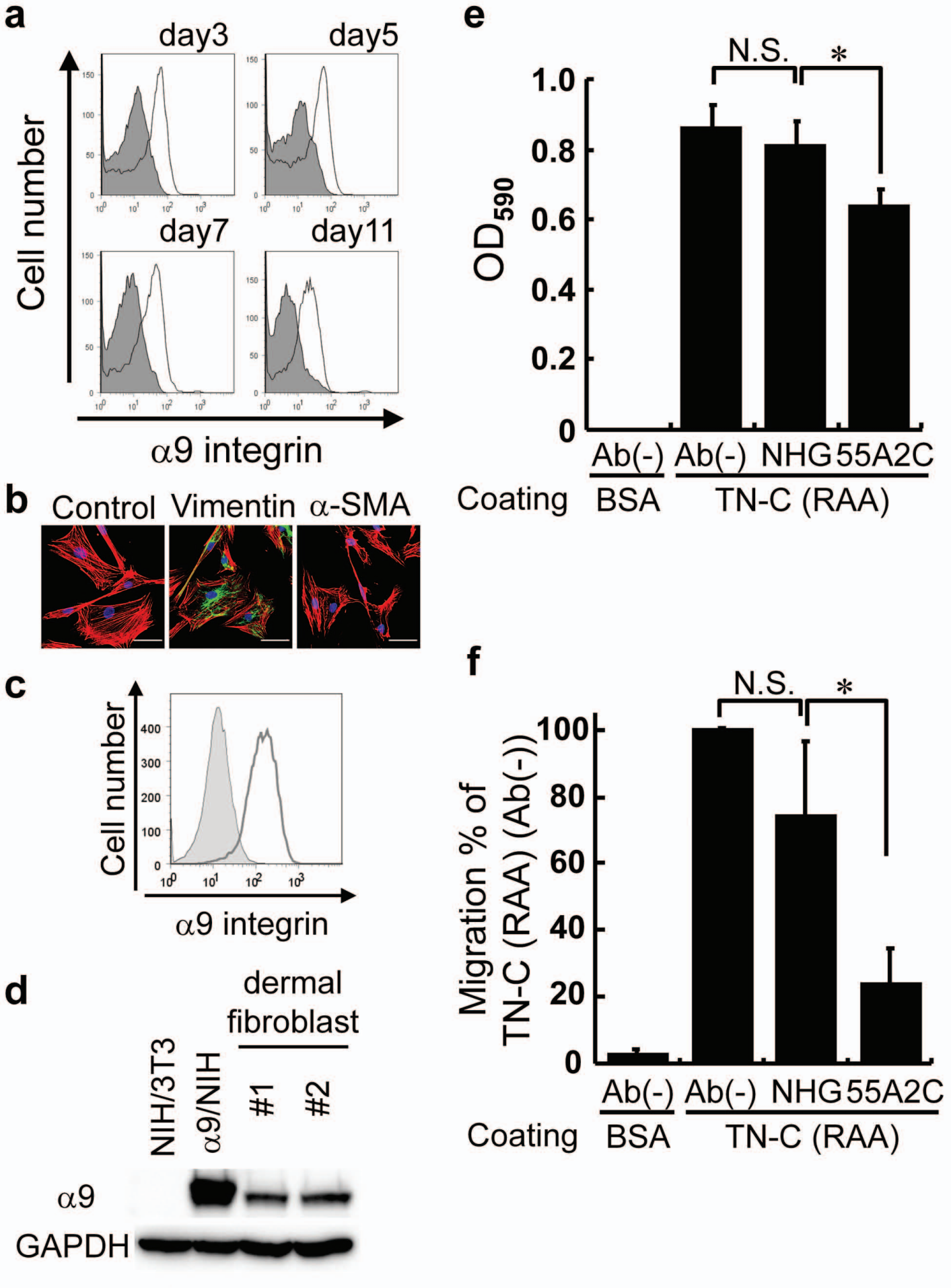
a
day3
day5
day7
day11
Cell number
α9 integrin
b
Control
Vimentin
α-SMA
c
Cell number
α9 integrin
d
NIH/3T3
α9/NIH
dermal fibroblast
#1
#2
α9
GAPDH
e
N.S.
*
OD590
1.0
0.8
0.6
0.4
0.2
0
Ab(-)
Ab(-)
NHG
55A2C
Coating
BSA
TN-C (RAA)
f
N.S.
*
Migration % of TN-C (RAA) (Ab(-))
100
80
60
40
20
0
Ab(-)
Ab(-)
NHG
55A2C
Coating
BSA
TN-C (RAA)

Figure 8

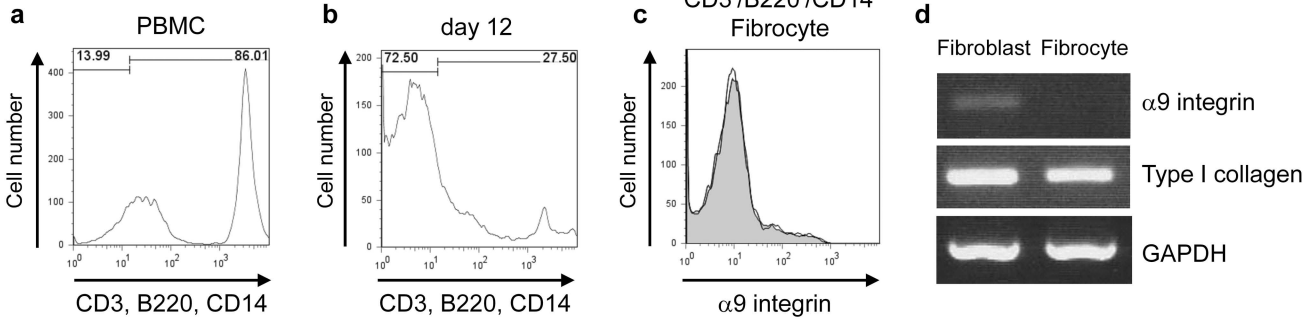
a
PBMC
13.99
86.01
Cell number
CD3, B220, CD14
b
day 12
72.50
27.50
Cell number
CD3, B220, CD14
c
CD3-/B220-/CD14-
Fibrocyte
Cell number
α9 integrin
d
Fibroblast
Fibrocyte
α9 integrin
Type I collagen
GAPDH

Figure 9